

# On the reduced electrical conductivity of radio-frequency sputtered doped ceria thin film by elevating the substrate temperature



Sanghoon Ji <sup>a</sup>, Jihwan An <sup>b</sup>, Dong Young Jang <sup>c</sup>, Youngseok Jee <sup>d</sup>, Joon Hyung Shim <sup>c</sup>, Suk Won Cha <sup>a, e, \*</sup>

<sup>a</sup> Graduate School of Convergence Science and Technology, Seoul National University, 145 Gwanggyo-ro, Yeongtong-gu, Suwon, 16229, South Korea

<sup>b</sup> Manufacturing Systems and Design Engineering Programme, Seoul National University of Science and Technology, 232 Gongneung-ro, Nowon-gu, Seoul, 01811, South Korea

<sup>c</sup> Department of Mechanical Engineering, Korea University, 145 Anam-ro, Seongbuk-gu, Seoul, 02841, South Korea

<sup>d</sup> Department of Mechanical Engineering, University of South Carolina, Columbia, SC, 29208, USA

<sup>e</sup> Department of Mechanical and Aerospace Engineering, Seoul National University, 1 Gwanak-ro, Gwanak-gu, Seoul, 08826, South Korea

## ARTICLE INFO

### Article history:

Received 20 August 2015

Received in revised form

9 December 2015

Accepted 9 December 2015

Available online 19 December 2015

### Keywords:

Electrical conductivity

Gadolinium-doped ceria

Substrate temperature

Radio frequency sputtering

Solid oxide fuel cell

## ABSTRACT

The electrical conductivity of ~200 nm-thick gadolinium-doped ceria (GDC) thin films deposited at various substrate temperatures by radio-frequency sputtering was evaluated in a temperature range of 400 °C–550 °C as an electrolyte for solid oxide fuel cells operated at low temperatures. Morphological, chemical, and crystalline properties were discussed to determine the electrical conductivity; in particular, the electrical conductivity of GDC thin film deposited at 300 °C was appreciably lower than that of GDC thin film deposited at 150 °C. The columnar grain boundaries and the reduced ceria formed during the sputtering process are considered as the major factors leading to the measured results.

© 2015 Elsevier B.V. All rights reserved.

## 1. Introduction

Solid oxide fuel cells (SOFCs), which adopt solid-state ceramics as electrolytes, are considered as a promising renewable energy device for the generation of electricity due to their high energy conversion efficiency, pollutant-free exhaust, and their simple balance of plant operation [1,2]. SOFCs, however, usually require excessively high operation temperatures (above 800 °C) to obtain sufficient cell performance. Although the development of thin film ceramic electrolytes over several decades has significantly reduced the operating temperatures of SOFCs, these lower operating temperatures have resulted in poor cell performance levels mainly owing to the drastic increase in the polarization resistance. This phenomenon is mostly attributed to the sluggish oxygen reduction reaction (ORR) activity at the cathode-electrolyte interface [3–5]. The use of thin film ceramic electrolyte materials with high surface

exchange coefficients in this respect is strongly required for fast ORR; at present, doped ceria is considered as a promising material to exhibit such a characteristic [6,7].

Radio-frequency (RF) sputtering to enable oxide targets has been actively employed to secure compositional reproducibility in the resulting oxide films, as the metal targets used in direct current sputtering are easily contaminated by the oxidizing source existed in the vacuum chamber [8,9]. Furthermore, the physicochemical properties of oxide films deposited via RF sputtering are highly adjustable by controlling process parameters such as the substrate temperature, bias voltage, and background gas, among others [10]. For instance, RF-sputtered doped ceria thin films for SOFCs operated at ~600 °C were deposited at elevated substrate temperatures to realize a high packing density onto a stabilized electrolyte, which successfully served as a protective layer between the stabilized zirconia electrolyte and the Co-containing perovskite cathode material [11,12]. Such efforts made thus far have mainly focused on the fabrication of a cathode interlayer to prevent the formation of undesirable products, whereas our understanding of the ion-conducting properties of RF-sputtered doped ceria thin film electrolytes for

\* Corresponding author. Department of Mechanical and Aerospace Engineering, Seoul National University, 1 Gwanak-ro, Gwanak-gu, Seoul, 08826, South Korea.

E-mail address: [swcha@snu.ac.kr](mailto:swcha@snu.ac.kr) (S.W. Cha).

low-temperature SOFCs remains insufficient [13].

In this study, doped ceria thin films deposited by using high-vacuum RF sputtering at various substrate temperatures were electrically characterized and investigated in terms of their morphological, chemical, and structural properties. In the substrate temperature regime selected here, the existence of hydroxyl species and dopants inside the film was not strikingly dependent on the variation of the substrate temperature. The elevation of the substrate temperature, on the other hand, led to changes in the morphology and stoichiometry and to changes in the crystallization properties; the effects of columnar grain boundaries and ceria reduction were considered as the major causes of the distinguishable electrical conductivity of the doped ceria thin films deposited at different substrate temperatures.

## 2. Experimental details

### 2.1. Thin film deposition

Gadolinium-doped ceria (GDC) thin films were deposited using a commercial sputtering machine (A-Tech System, South Korea) with a customized rotational and heating unit. The base pressure was maintained at  $\sim 1.0 \times 10^{-4}$  Pa, and the background pressure was kept at 1.3 Pa during the deposition process. The target-to-substrate distance was 75 nm, and the substrate was rotated at 4 rpm to enhance the thickness uniformity in the lateral direction. The reactive sputtering gas was a mixture of Ar and O<sub>2</sub> at a volumetric ratio of 80:20. The RF magnetron power of the sputtering gun was 50 W. A copper backing plate-bonded two-inch GDC disk pellet with 10 mol% of Gd<sub>2</sub>O<sub>3</sub> was used as the target. The substrate was heated at a ramping rate of 10°C/min after the background pressure became saturated, which was passively cooled as soon as the RF sputtering gun was discharged.

### 2.2. Thin film characterization

The microstructure of the GDC thin films was investigated by the combination of a focused ion beam, a manufacturing process capable of digging for samples, and the two electron microscopic methods of field-emission scanning electron microscopy (FIB/FE-SEM) using a Quanta 3D FEG instrument (FEI Company, Netherlands) and transmission electron microscopy (TEM) using a Tecnai G2 F30 S-TWIN instrument (FEI Company, Netherlands). The chemical properties of the GDC thin films were investigated by X-ray photoelectron spectroscopy (XPS) using an AXIS His instrument (Kratos Analytical, UK), and possible surface contaminants originating from the ambient air were eliminated by means of 150 eV Ar-ion etching for 30 s prior to the analysis. The crystalline properties of GDC thin films were investigated by X-ray diffraction (XRD) using an X'Pert Pro instrument (PANalytical, Netherlands) with Cu K $\alpha$  radiation in the symmetrical  $\theta/2\theta$  scan mode.

### 2.3. Electrical conductivity measurements

A Si(100) wafer with a SiO<sub>2</sub> additional layer 200 nm-thick was used as the electronically insulative substrate for cross-plane electrical conductivity measurements. Sputtered dense Pt thin film with a thickness of 100 nm was used as both the bottom and top electrodes [14]. The Pt/as-prepared GDC/Pt thin film assemblies coated onto the SiO<sub>2</sub>-coated Si wafer were heated to the measurement temperatures on a conductive heating unit. The relative humidity in ambient air at room temperature (RT) was adjusted to 30%. Electrochemical impedance spectroscopy was carried out at the open-circuit voltage by bringing micro-tips into contact with the Pt electrodes, and impedance behaviors independent of the

variation of the bias voltage were used to determine the total conductivity in conjunction with the oxygen ionic and electronic conductivities.

## 3. Results and discussion

### 3.1. Morphological and electrical analysis

FE-SEM cross-sectional imaging of the FIB-prepared GDC thin films deposited at various substrate temperatures ranging from RT to 300 °C determines that the apparent growth rate of the GDC thin films gradually decreases as the substrate temperature is increased. These results were  $\sim 55$ ,  $\sim 42$ , and  $\sim 35$  nm/h at RT, 150, and 300 °C, respectively. This tendency of the apparent growth rate to decrease with an increase in the substrate temperature is attributable to microstructural densification caused by the enhanced mobility of the bombarded Gd/Ce/O adatoms on the top of the substrate. Thus, we fixed the apparent thickness of the resulting GDC thin films to alleviate the morphological effects of the variation in the vertical growth direction; in this case, the selected thickness was  $\sim 200$  nm. The GDC thin films 200 nm-thick deposited at RT, 150, and 300 °C are hereafter denoted as the GDC-RT, GDC-150, and GDC-300, respectively [15]. It is generally known that the elevation of the substrate temperature during sputtering leads to an increase in the grain size due to the enhancement of the adatom mobility onto the substrate [16]. In the same vein, the grain sizes of the GDC thin films fabricated in this study increase as the substrate temperature is increased, as confirmed through microscopic top-view imaging, which is regarded as an appropriate means by which to observe the granular films [17–19]: the average grain sizes of the GDC-RT, GDC-150, and GDC-300 are  $\sim 30$ ,  $\sim 34$ , and  $\sim 50$  nm, respectively (Fig. 1 a,b, and c). There is little difference in the grain size between GDC-RT and GDC-150, although the substrate temperatures for these two films are very different. This may have occurred because the actual deposition temperature of GDC-RT was far higher than RT by self-heating due to the collisions between the substrate surface and the bombarded Gd/Ce/O atoms. Some may expect that the increase in the grain size will reduce the grain boundary density so that the electrical conductivity of the GDC thin film would increase by mitigating the resistive effects on the ion conductance at the grain boundary regions via what are known as ionic blocking effects [20]. Nonetheless, the enhancement of electrical conductivity caused by the reduction of the ionic blocking effects may be valid when the size of the crystallites (or GDC grains) is large enough to have a great effect on the degree of the dopant ion (or Gd ion) segregation [21].

TEM cross-sectional imaging of FIB-prepared GDC-150 and GDC-300 pertaining to different zones in the growth model proposed by Thornton [22] shows that almost no columnar grain boundaries can be seen clearly in GDC-150 within Zone 1, while GDC-300 within Zone T has a relatively large number of distinguishable columnar grain boundaries inside the film (Fig. 2 a and b). This observation of further developed columnar grain boundaries with differently oriented lattices in GDC-300 can be explained through the growth characteristics in a transition state presented in these structure zone diagrams, indicating that the elevation of the substrate temperature under a high vacuum contributes to the notable microstructural change of the thin films. Many more dislocations observed in GDC-300 could result in the reduction of the electrical conductivity by narrowing the ionic paths (or hindering the ionic conduction) [23]. In fact, the aforementioned morphological investigation is in good agreement with the results of the electrical conductivity measurements (Fig. 3); the electronic conductivity herein is assumed to be negligible because the analysis environment is a highly oxidizing atmosphere. Although the activation

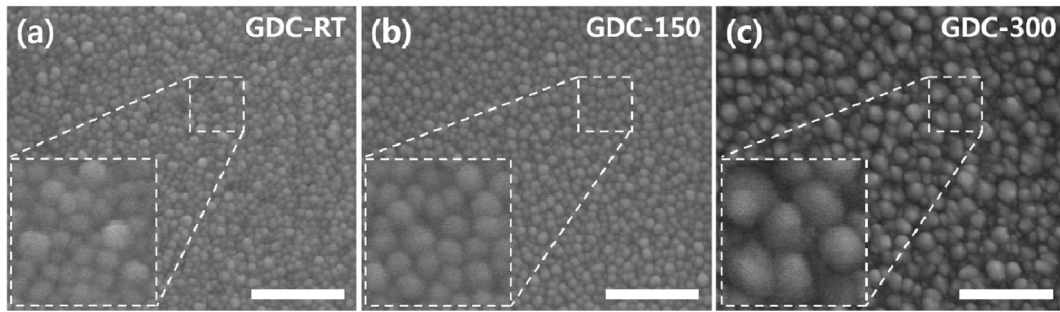


**Fig. 1.** Field emission scanning electron microscopy top-view images of 200 nm-thick gadolinium-doped ceria (GDC) films deposited at (a) room temperature (RT), (b) 150 °C, and (c) 300 °C, which are denoted as the GDC-RT, GDC-150, and GDC-300, respectively (scale bar = 400 nm).

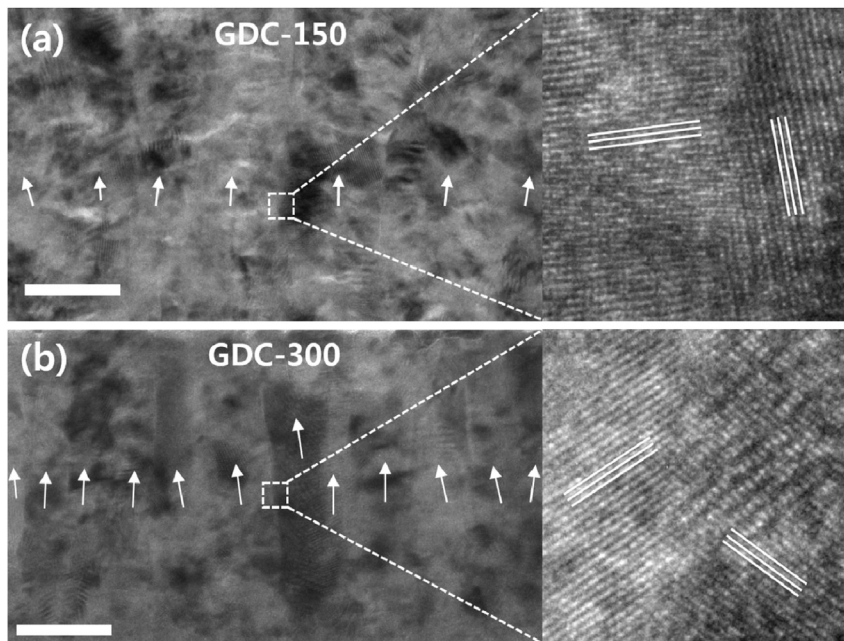


**Fig. 2.** Focused ion beam-prepared transmission electron microscopy cross-sectional images of GDC-150 and GDC-300 (scale bar = 40 nm). Ascending arrows marked in lower resolution images indicate developed individual columns inside the films.

energy, i.e., the slope of electrical conductivity (Y-axis value) versus the operation temperature (X-axis value), is nearly identical to  $\sim 0.95$  eV, the difference in the electrical conductivity levels is considerable. These experimental results above all indicate that the elevation of the substrate temperature affecting the density of the columnar grain boundaries must be carefully manipulated to obtain high enough electrical conductivity in GDC thin films when they are used as an oxygen ion conductor. Meanwhile, the GDC thin films fabricated in this study exhibit higher conductivity than the well-defined YSZ film but lower electrical conductivity (and higher activation energy) than GDC thin films prepared by other physical vapor deposition methods, which may be due to the absence of a post-deposition heat treatment, which is generally regarded as an effective means of providing sufficiently high electrical conductivity by crystallizing and densifying electrolyte thin films deposited at low temperatures [19,24–26].

### 3.2. Chemical and structural analysis

The XPS peak intensities of Ce 3d show that the elevation of the substrate temperature results in the formation of reduced GDC thin films which deviate from the chemical formula of  $\text{CeO}_2$  (Fig. 4a).

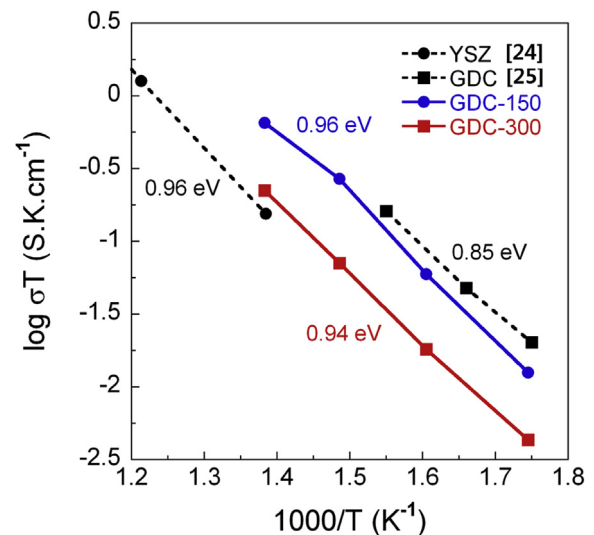


**Fig. 3.** Electrical conductivity of GDC-150 and GDC-300, and other well-prepared yttria-stabilized zirconia (YSZ) and GDC thin films deposited by physical vapor deposition.

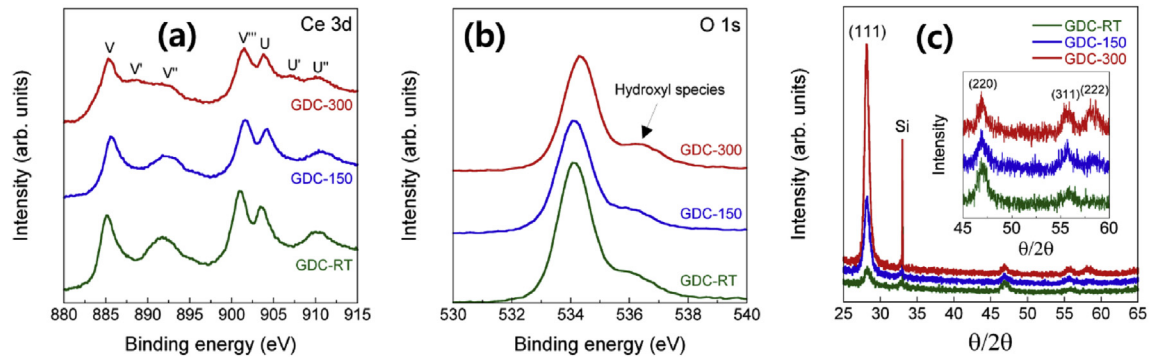


**Fig. 4.** X-ray photoelectron spectroscopy spectra for (a) Ce 3d and (b) O 1s peak intensities and (c) X-ray diffractograms for (111), (220), (311), and (222) peak intensities of GDC-RT, GDC-150, and GDC-300.

Based on the fact that ceria can be vigorously reduced at high temperatures under low oxygen partial pressures [27], we consider that our process condition of a heated substrate along with a high vacuum brought about the formation of such non-stoichiometric GDC thin films. In this regard, we also believe that the lattice-oxygen extraction originating from ceria reduction could reduce the electrical conductivity, with the subsequent destruction of the oxygen vacancy structure [28]. The XPS peak intensities of O 1s show that hydroxyl species, which would affect the protonic conduction through the solid oxide electrolytes, exist in all GDC thin films (Fig. 4b). Because the base pressure during the sputtering process was maintained in a high vacuum (below  $1.0 \times 10^{-4}$  Pa) and no hydrogen-containing sources were supplied inside the chamber, it is strongly believed that the formation of hydroxyl species in the GDC thin films is likely due to the spontaneous chemical reaction between the oxygen ions already existing inside the GDC thin films and water molecules which are passively supplied from ambient air [29]. Nevertheless, there is no large discrepancy in the peak intensity at the binding energy ( $\sim 536.5$  eV) corresponding to hydroxyl species, which indicates that the substrate temperature is not the parameter which strongly influences the formation of hydroxyl species in GDC thin films. The XPS quantitative analysis results show that the Gd doping levels of all GDC thin films range from 10.5% to 11.4%, indicating that the Gd doping level is not the major factor which influences the electrical conductivity [30,31]. Meanwhile, the XRD diffractograms (Fig. 4c) show that the elevation of the substrate temperature notably enhances the polycrystalline characteristics of GDC thin films; in particular, the (111) peak, leading to the best electrical conductivity of the oxygen ion conductors, increases more sharply compared to other diffraction peaks [24]. This structural analysis result therefore indicates that the crystallinity is not the most influential factor determining the electrical conductivity of GDC thin films.

#### 4. Conclusion

We investigated the electrical conductivity and material properties of RF-sputtered GDC thin films deposited at various substrate temperatures under high-vacuum conditions for SOFCs operated at low temperatures. In spite of the better crystalline properties in terms of the oxygen ion conduction, interestingly, the structural dislocation originating from the development of columnar GDC grain boundaries and the ceria reduction caused by the condition of a high temperature and a low oxygen partial pressure significantly lowered the electrical conductivity when the substrate temperature was elevated. We therefore emphasize that both the structural

compatibility and chemical integrity must be considered as major factors which determine the electrical conductivity of dense GDC thin films deposited by RF sputtering at elevated substrate temperatures.

#### Acknowledgments

This work was supported by the Global Frontier R&D Program on Center for Multiscale Energy System funded by the National Research Foundation under the Ministry of Science, ICT & Future Planning, Korea (2015M3A6A7065442), and partially supported by the National Research Foundation (NRF) of Korea grant funded by the Korea government (2013R1A1A2A10065234 and 2011-0029576). In addition, Jihwan An acknowledges partial support from the NRF of Korea grant funded by the Korea government (NRF-2015R1D1A1A01058963).

#### References

- [1] B.C. Steele, A. Heinzl, *Nature* 414 (2001) 345.
- [2] A.B. Stambouli, E. Traversa, *Renew. Sust. Energ. Rev.* 6 (2002) 433.
- [3] S. Ji, I. Chang, Y.H. Lee, M.H. Lee, S.W. Cha, *Thin Solid Films* 539 (2013) 117.
- [4] S. Ji, G.Y. Cho, W. Yu, P.C. Su, M.H. Lee, S.W. Cha, *ACS Appl. Mater. Interfaces* 7 (2015) 2998.
- [5] J. An, J.H. Shim, Y.B. Kim, J.S. Park, W. Lee, T.M. Gür, F.B. Prinz, *MRS Bull.* 39 (2014) 798.
- [6] S. Ji, I. Chang, Y.H. Lee, J. Park, J.Y. Paek, M.H. Lee, S.W. Cha, *Nanoscale Res. Lett.* 8 (2013) 48.
- [7] S. Ji, I. Chang, G.Y. Cho, Y.H. Lee, J.H. Shim, S.W. Cha, *Int. J. Hydrog. Energ.* 39 (2014) 12402.
- [8] S. Ji, W.H. Tanveer, W. Yu, S. Kang, G.Y. Cho, S.H. Kim, J. An, S.W. Cha, *Beilstein J. Nanotechnol.* 6 (2015) 1805.
- [9] S. Ji, Y.H. Lee, T. Park, G.Y. Cho, S. Noh, Y. Lee, M. Kim, S. Ha, J. An, S.W. Cha, *Thin Solid Films* 591 (2015) 250.
- [10] D. Beckel, A. Bieberle-Hütter, A. Harvey, A. Infortuna, U. Muecke, M. Prestat, J. Rupp, L. Gauckler, *J. Power Sources* 173 (2007) 325.
- [11] W. Wu, X. Wang, Z. Liu, Z. Zhao, D. Ou, B. Tu, M. Cheng, *Fuel Cells* 14 (2014) 171.
- [12] F. Fonseca, S. Uhlenbruck, R. Nedélec, H. Buchkremer, *J. Power Sources* 195 (2010) 1599.
- [13] H. Huang, M. Nakamura, P. Su, R. Fasching, Y. Saito, F.B. Prinz, *J. Electrochem. Soc.* 154 (2007) B20.
- [14] D.Y. Jang, H.K. Kim, J.W. Kim, K. Bae, M.V. Schlupp, S.W. Park, M. Prestat, J.H. Shim, *J. Power Sources* 274 (2015) 611.
- [15] V. Ng, J. Hu, A. Adeyeye, J. Wang, T. Chong, *J. Appl. Phys.* 91 (2002) 7206.
- [16] S.H. Cho, *Trans. Electr. Electron. Mater.* 10 (2009) 185.
- [17] J. Bae, S. Hong, B. Koo, J. An, F.B. Prinz, Y.-B. Kim, *J. Eur. Cera. Soc.* 34 (2014) 3763.
- [18] J.S. Park, J. An, M.H. Lee, F.B. Prinz, W. Lee, *J. Power Sources* 295 (2015) 74.
- [19] S. Heiroth, R. Frison, J.L. Rupp, T. Lippert, E.J.B. Meier, E.M. Gubler, M. Döbeli, K. Conder, A. Wokaun, L.J. Gauckler, *Solid State Ionics* 191 (2011) 12.
- [20] H. Huang, T.M. Gür, Y. Saito, F. Prinz, *Appl. Phys. Lett.* 89 (2006) 3107.
- [21] E. Gourba, P. Briois, A. Ringuédé, M. Cassir, A. Billard, *J. Solid State Chem.* 8 (2004) 633.
- [22] J.A. Thornton, *J. Vac. Sci. Technol. A* 4 (1986) 3059.

- [23] F. Ye, C.Y. Yin, D.R. Ou, T. Mori, *Prog. Nat. Sci. Mater. Int.* 24 (2014) 83.
- [24] J.H. Joo, G.M. Choi, *Solid State Ionics* 177 (2006) 1053.
- [25] J.H. Joo, G.M. Choi, *J. Eur. Ceram. Soc.* 27 (2007) 4273.
- [26] S. Heiroth, T. Lippert, A. Wokaun, *Appl. Phys. A Mater. Sci.* 93 (2008) 639.
- [27] J. Fierro, J. Soria, J. Sanz, J. Rojo, *J. Solid State Chem.* 66 (1987) 154.
- [28] J.L. Rupp, A. Infortuna, L.J. Gauckler, *J. Am. Ceram. Soc.* 90 (2007) 1792.
- [29] H. Kishimoto, N. Sakai, K. Yamaji, T. Horita, M.E. Brito, H. Yokokawa, *ECS Trans.* 13 (2008) 105.
- [30] H.J. Avila-Paredes, C.T. Chen, S. Wang, R.A. De Souza, M. Martin, Z. Munir, S. Kim, *J. Mater. Chem.* 20 (2010) 10110.
- [31] Y.L. Kuo, C. Lee, Y.S. Chen, H. Liang, *Solid State Ionics* 180 (2009) 1421.